COVER SHEET

THERMAL TWEEZERS FOR SURFACE MANIPULATION WITH NANO-SCALE RESOLUTION

Dmitri K. Gramotnev, Daniel R. Mason, Galina Gramotnev, and Anthony J. Rasmussen

Applied Optics Program, School of Physical and Chemical Sciences, Queensland University of Technology, GPO Box 2434, Brisbane, QLD 4001, Australia

d.gramotnev@qut.edu.au

ABSTRACT

In this letter, we demonstrate that random Brownian forces can be used for effective trapping and manipulation of nanoparticles and molecules on surfaces in the presence of strong temperature modulation. Substantial (~ 2 orders of magnitude) increase in the modulation of particle concentration (trapping efficiency) compared to thermophoresis in a bulk medium is predicted and explained by a periodic potential of interaction between a particle/molecule and the crystalline surface. As a result, a new nanofabrication and manipulation technique for creating optically-induced complex surface structures with nano-scale resolution below tens of nanometers is proposed and developed.

Optical tools for manipulation and trapping of microscopic particles (optical tweezers) is one of the major areas of modern optics, and a multi-million dollar industry with extensive applications in medicine, life science, micro-machines, new sensors and measurement techniques, etc. [1-5]. However, optical manipulation of particles with dimensions below ~ 100 nm is difficult, because of dominating random Brownian forces [6-8].

One of the possibilities to overcome this difficulty has been related to using light near resonance absorption [9-12]. A substantial increase in the trapping gradient force has been predicted (~ 50-fold [9] and up to ~ 10000-fold [11,12]). This may certainly improve the situation with trapping and manipulation of nano-particles below ~ 100 nm diameter. However, the effect is highly sensitive to shape and structure of the particles [11], and it requires specially tuned optical tweezers. While this may be a good technique for sorting particles [11,12], it is hardly appropriate for parallel nanofabrication with simultaneous manipulation of a large number of particles that may slightly differ in properties, size and shape. Resonant trapping occurs near a strong absorption line, which does not always exist in the convenient range of frequencies. Strong absorption is expected to result in significant heating effects and heat destruction of the particles. In addition, none of the current optical manipulation techniques has specifically been designed for manipulation of nano-particles on surfaces and interfaces, which is an essential problem in nanofabrication and nanotechnology.

On the other hand, strong temperature gradients may result in anisotropic diffusion of particles/molecules in a bulk medium. This effect is called thermophoresis [13,14]. It is characterized by the preferred direction of diffusion from hot to cold regions. A similar effect can also be expected to occur for nano-particles/molecules on surfaces in the presence of temperature modulation. The particles/molecules should accumulate in the cold regions on the surface, which means the existence of a net gradient trapping force in the direction from the hot to cold regions. This diffusive trapping force is related to stronger random Brownian motion of particles in the hot regions. As a result, the probability for particles to escape the hot regions is larger than that for the cold regions. Therefore there

is a net translational momentum transferred to the particles from the hot to cold regions, originating from the lattice oscillations (phonons) in the substrate.

The aim of this letter is to demonstrate that random Brownian forces can be used for effective trapping and manipulation of nanoparticles and molecules on surfaces in the presence of strong temperature modulation. Substantial (~ 2 orders of magnitude) increase in the modulation of particle concentration (trapping efficiency) compared to thermophoresis in a bulk medium is predicted and analyzed. As a result, a new nanofabrication and manipulation technique for creating complex surface structures with nano-scale resolution below tens of nanometers is proposed and developed.

There is a fundamental difference between thermophoresis in a bulk medium [13,14] and on a flat surface. This is because particles/molecules on the surface move in a periodic or random two-dimensional potential due to their interaction with, for example, a periodic lattice of the substrate [15-18]. As we will see below, this may result in modulation of particle/molecule concentration on the surface that is several orders of magnitude larger than that achievable in a bulk medium [13,14].

Thermophoresis on surfaces can thus be used as a new technique (that we will call thermal tweezers) for nanofabrication, manipulation and trapping of nanoparticles and molecules. Strong temperature gradients on the surface can be produced by the holographic approach, e.g., by interference of two or more laser pulses (Fig. 1). Therefore, any interference pattern (holographic image) can be reproduced (recorded) by means of the resultant particle/molecule re-distribution on the surface. This opens new unique opportunities for parallel manipulation and fabrication with nano-scale (see below) resolution, using a large number of particles/molecules on large surface areas.

Contrary to the optical tweezers, the trapping efficiency in the thermal tweezers increases with decreasing size of the particles/molecules. This is because thermal tweezers use random Brownian motion as the primary source of the gradient trapping force, and such motion intensifies with decreasing size of the particles.

To demonstrate the major effects and nanofabrication capabilities associated with thermal tweezers, we use the general and physically intuitive model based on the Markovian Langevin equation [15-18]:

$$m\frac{d^2\mathbf{r}}{dt^2} = -m\gamma\frac{d\mathbf{r}}{dt} - \nabla V(\mathbf{r}) + \xi_{\mathbf{r}}(t)\,. \tag{1}$$

Here, m is the mass of the particle/molecule, $\mathbf{r} = \mathbf{i}x + \mathbf{j}y$ is its two-dimensional position vector on the surface. The particles are assumed to move in a periodic potential due to their interaction with the square crystal lattice of the substrate with the period a:

$$V(\mathbf{r}) = \frac{V_0}{2}\left[\cos\left(\frac{2\pi x}{a}\right) + \cos\left(\frac{2\pi y}{a}\right)\right], \tag{2}$$

$\xi_{\mathbf{r}}(t)$ is the random Brownian force resulting from the δ-correlated Gaussian thermal fluctuations:

$$\left\langle \xi_i(t)\xi_j(t')\right\rangle = \frac{2\gamma k_b T(x)}{m}\delta_{ij}\delta(t-t')\,, \tag{3}$$

γ is the effective coefficient of friction for the particle, k_b is the Boltzmann constant, $T(x) = T_0 + \Delta T\cos^2(\pi x/\lambda)$ is the temperature on the surface with the period λ along the x-axis and uniform along the y-axis.

Numerical solution of Eq. (1) for one particle/molecule gives the position of this particle after a specified time interval. Repeating this procedure for a large number of particles gives the probability density function $\rho(x)$ that determines the probability $dP = \rho(x)dx$ to find the particle/molecule within the interval dx. This function fully determines the distribution of particles on the surface after the specified time interval. It is assumed to be normalized by the condition: $\int_0^{\lambda}\rho(x)dx = 1$. The initial position of each particle is chosen randomly within a λ × λ square with the periodic boundary conditions and the sides parallel to the x- and y-axes.

The results are presented in Figs. 2 and 3 showing substantial re-distribution of particles/molecules on the surface. Fig. 2 demonstrates that increasing depth of the potential wells V_0 (Eq. (2)) results in a rapid increase of modulation of particle concentration by thermal tweezers. For example, the ratios of the maximal to minimal steady-state probability densities (i.e., the maximal to minimal particle concentrations) are equal to (71 ± 12), (6.6 ± 0.5), (2.18 ± 0.02) for $V_0 = k_bT/0.15$, $V_0 = k_bT/0.4$, and $V_0 = 0$, respectively (Fig. 2). As indicated above, this is one of the major differences between the thermal tweezers and bulk thermophoresis [13,14] (compare the thick solid curve in Fig. 2b with all other curves). Interestingly, this modulation enhancement is achieved without increasing gradient force that is determined by thermal phonons in the substrate. The enhancement occurs because of the additional suppression of diffusion in the cold regions (due to trapping in the wells with $V_0 > k_bT$), which makes it even more difficult for the particles to leave these regions. On the other hand, the same mechanism also results in increasing relaxation time τ for the steady-state particle distribution to be reached (Fig. 2).

It has also been shown that if in Fig. 2a the coefficient of friction is increased 4 times (i.e., up to $\gamma = 3.5\times10^{10}$ s^{-1}), then the maximums of the probability density (in the cold regions) change only insignificantly from (14.7 ± 0.2) nm^{-1} for Fig. 2a to (13.9 ± 0.2) nm^{-1} for the 4 times larger friction. At the same time, ratio of the maximal to minimal steady-state probability densities reduce noticeably from (71 ± 12) to (49 ± 6), and the typical evolution times increase ~ 3 times.

Fig. 3 shows that increasing temperature modulation results in a significant increase of the steady-state modulation of particle concentration on the surface and decrease of the relaxation time τ (for example, for the upper curves in Fig. 3, τ = (118 ± 6) ns, (148 ± 8) ns, (270 ± 40) ns for ΔT = 400 K, 300 K, 200 K, respectively). This is because increasing ΔT results in increasing size of the hot regions, diffusion rate, and gradient trapping force. The relaxation in the cold regions takes substantially longer than in the hot regions (Fig. 3). This is because diffusion rate in the hot regions is significantly higher.

One of the important aspects of curves 4 and 5 in Fig. 2a is the existence of two maximums of the probability density on both sides of each cold region. These maxima may only occur in the non-steady-state regime when the particles rapidly diffuse from the hot regions, but do not have enough time to reach the cold regions (because of much slower diffusion at lower temperatures). This effect increases with increasing friction and leads to a superresolution technique in thermal tweezers (Fig. 4).

Fig. 4a reproduces curve 1 from Fig. 2a with only one maximum per period of the temperature modulation λ (no superresolution). The superresolution can be achieved as follows. A large temperature modulation is applied to a uniform particle distribution on the surface with sufficiently deep potential wells to suppress diffusion in the cold areas. The resultant typical size distribution (after t = 200 ns) is shown in Fig. 4b. No noticeable diffusion has occurred in the cold regions, and two strong concentration maxima have emerged almost exactly in between the cold and hot regions (Fig. 4b).

Shifting the interference pattern of the laser pulses by π, we interchange the hot and cold regions on the surface. Allowing the system to evolve for another 200 ns, results in effective diffusion of particles from the former cold (currently, hot) regions into the same maxima between the hot and cold regions (Fig. 4c).

Reduce the background temperature T_0, in order to increase the regions with suppressed diffusion. Shift the interference pattern further by $\approx \pi/2$, so that the hot regions coincide with every second concentration maximum in Fig. 4c. Another 600 ns of evolution results in each such maximum splitting into two, while the maxima in the cold regions are left unchanged (Fig. 4d). This results in three maxima (instead of one – Fig. 4a) within one period of the temperature modulation λ = 316.4 nm (Fig. 4d). The widths of these maxima are ~ 35 – 40 nm.

As a result, thermal tweezers with laser pulses in the visible range of spectrum can be used for nanofabrication of surface elements with dimensions of a few tens of nanometers. Further increase of the resolution can be achieved by illuminating a thin metal film from the dielectric substrate (Fig. 1b).

This results in reducing period of the temperature modulation on the film surface, and thus increasing resolution proportionally to the refractive index of the substrate. In addition, interaction between the particles (i.e., their coagulation into clusters) should lead to a significant increase in height and sharpness of the concentration maxima in the cold regions. Indeed, once the particles coagulate, they become less mobile and form stationary potential wells for other particles, and this is much more likely to occur in the cold regions with larger particle concentration and smaller probability for thermal fragmentation of the clusters. Therefore, the results obtained in this paper are rather applicable at small surface concentrations of particles, while at large concentrations they only present lower estimates of the concentration modulation and spatial resolution.

It has also been assumed that the temperature modulation ΔT is time independent. In practice, this is usually not the case, and the temperature modulation typically lasts for a period of time that is of the order of the pulse duration (which should be in the picosecond or nanosecond range, to ensure the considered temperature modulations). Therefore, multiple pulse treatment could be required.

Thus, a new nanofabrication technique – thermal tweezers – has been proposed and described for parallel nanofabrication/manipulation (with the resolution as good as tens of nanometers or better) of any surface structures obtainable by the holographic approach using laser pulses in the visible range of frequencies. Combined with laser ablation and deposition, thermal tweezers may pave the way for new all-optical nanofabrication processes in nanotechnology and surface science.

References

1. A. Ashkin, *Proc. Natl. Acad. Sci. USA*, **94**, 4853-4860 (1997).

2. A. Ashkin, *IEEE J. Select. Top. Quantum Elec*., **6**, 841-856 (2000).

3. M. J. Lang, S. M. Block, Resource Letter: LBOT-1: Laser-based optical tweezers. *Am. J. Phys.*, **71**, 201-215 (2003).

4. J. E. Molloy, M. J. Padgett, *Contemporary Physics*, **43**, 241-258 (2002).

5. K. C. Neuman, S. M. Block, *Rev. Sci. Instrum*., **75**, 2787-2809 (2004).

6. K. Okamoto, S. Kawata, *Phys. Rev. Lett*., **83**, 4534-4537 (1999).

7. A. Simon, A. Libchaber, *Phys. Rev. Lett*., **68**, 3375-3378 (1992).

8. S. A. Tatarkova, W. Sibbett, K. Dholakia, *Phys. Rev. Lett*., **91**, 038101 (2003).

9. R. R. Agayan, F. Gittes, R. Kopelman, C. F. Schmidt, *Appl. Optics*, **41**, 2318-2327 (2002).

10. J. R. Arias-Gonzalez, M. *J.* Nieto-Vesperinas, *J. Op. Soc. Am*. A, **20**, 1201-1209 (2003).

11. T. Iida, H. Ishihara, *Phys. Rev. Lett*., **90**, 057403 (2003).

12. T. Iida, H. Ishihara, *J. Luminescence*, **108**, 351-354 (2004).

13. I. Goldhirsch, D. Ronis, *Phys. Rev. A*, **27**, 1616-1634 (1983).

14. I. Goldhirsch, D. Ronis, *Phys. Rev. A*, **27**, 1635-1656 (1983).

15. T. Ala-Nissila, S. C. Ying, *Progress in Surface Science*, **39**, 227-323 (1992).

16. J. M. Sancho, A. M. Lacasta, K. Lindenberg, I. M. Sokolov, A. H. Romero, *Phys. Rev. Lett*., **92**, 250601 (2004).

17. A. M. Lacasta, J. M. Sancho, A. H. Romero, I. M. Sokolov, K. Lindenberg, *Phys. Rev.* E, **70**, 051104 (2004).

18. J. Kallunki, M. Dube, T. Ala-Nissila, *Surface Science*, **460**, 39-48 (2000).

Figure Captions:

Figure 1. Structures for thermal tweezers. Nano-particles on the surface of a thin metal film deposited onto a dielectric substrate. The arrows represent two laser pulses producing an interference pattern and the periodic temperature modulation on the surface of the film. (a) The pulses are incident onto the free surface of the film. (b) The interfering pulses are incident through the dielectric substrate (the temperature modulation at the free surface of the film is produced primarily due to heat conduction through the thin film).

Figure 2. The probability density functions $\rho(x)$ averaged over the final positions of 50,000 independent particles/molecules within the $\lambda \times \lambda$ square on the surface. λ = 316.4 nm (half-the-wavelength for a He-Ne laser), T_0 = 300 K, ΔT = 400 K, m = 100 a.u., a = 0.2 nm, $\gamma = 8.8\times10^9$ s^{-1} [15-18]. (a) $V_0 = k_bT_0/0.15$ for different evolution times: 1) t = 500 ns, 2) t = 200 ns, 3) t = 100 ns, 4) t = 50 ns, 5) t = 25 ns. (b) $V_0 = k_bT_0/0.4$, 1) t = 15 ns, 2) t = 5 ns, 3) t = 2.5 ns, 4) t = 1 ns; the thick solid curve is obtained using 100,000 independent particles, and corresponds to the steady-state probability density at V_0 = 0 (two-dimensional bulk thermophoresis). Dashed horizontal lines represent the steady-state maximal probability densities in the cold regions for (a) $V_0 = k_bT/0.15$ and (b) $V_0 = k_bT/0.4$.

Figure. 3. The time evolution of the probability density in the cold (the upper curves) and hot (the lower curves) regions at different temperature modulations ΔT: 400 K (solid), 300 K (dotted), 200 K (dash-and-dotted); the other parameters are the same as for Fig. 2a. The error bars on the upper curves (concentration maximums) show the typical standard errors of the mean for the calculated points. Curve fitting was done assuming exponential dependencies.

Figure 4. Superresolution technique in thermal tweezers. (a) The probability density function $\rho(x)$ identical to curve 1 in Fig. 2a (no superresolution). (b) $\rho(x)$ resulting from applying thermal tweezers to the uniform distribution of 50,000 non-interacting particles (in the $\lambda \times \lambda$ square with the periodic boundary conditions) at T_0 = 500 K, $V_0 = 500k_b/0.065$, ΔT = 800 K, λ = 316.4 nm, m = 100 a.u.,

a = 0.2 nm, $\gamma = 2.3\times10^{10}$ s^{-1} [15-18], and the evolution time t = 200 ns. (c) $\rho(x)$ obtained from the particle distribution in (b) by shifting the temperature modulation pattern by π and allowing the system to evolve for another 200 ns. (d) $\rho(x)$ obtained from the particle distribution in (c) by making T_0 = 300 K, further shifting the temperature modulation by $\approx \pi/2$ (so that the hot regions coincide with every second maximums in (c)), and allowing the system to evolve for 600 ns.

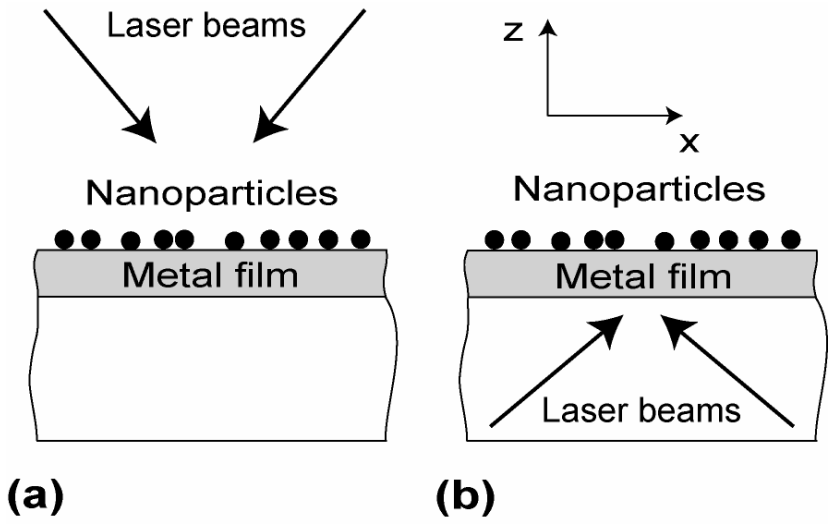

Figure 1. Structures for thermal tweezers. Nano-particles on the surface of a thin metal film deposited onto a dielectric substrate. The arrows represent two laser pulses producing an interference pattern and the periodic temperature modulation on the surface of the film. (a) The pulses are incident onto the free surface of the film. (b) The interfering pulses are incident through the dielectric substrate (the temperature modulation at the free surface of the film is produced primarily due to heat conduction through the thin film).

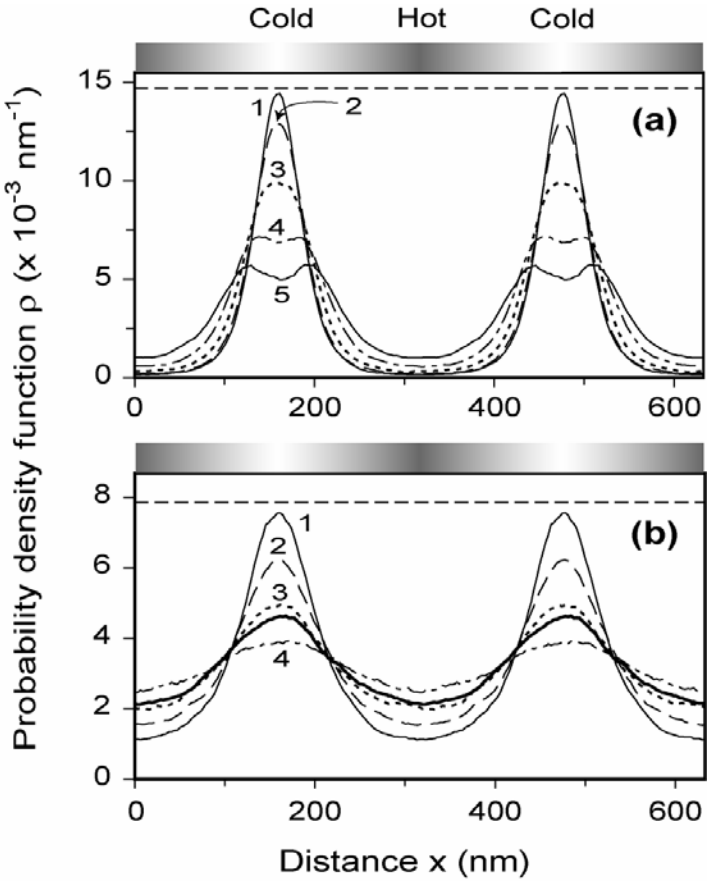

Figure 2. The probability density functions $\rho(x)$ averaged over the final positions of 50,000 independent particles/molecules within the $\lambda \times \lambda$ square on the surface. λ = 316.4 nm (half-the-wavelength for a He-Ne laser), T_0 = 300 K, ΔT = 400 K, m = 100 a.u., a = 0.2 nm, $\gamma = 8.8\times10^9$ s^{-1} [15-18]. (a) $V_0 = k_bT_0/0.15$ for different evolution times: 1) t = 500 ns, 2) t = 200 ns, 3) t = 100 ns, 4) t = 50 ns, 5) t = 25 ns. (b) $V_0 = k_bT_0/0.4$, 1) t = 15 ns, 2) t = 5 ns, 3) t = 2.5 ns, 4) t = 1 ns; the thick solid curve is obtained using 100,000 independent particles, and corresponds to the steady-state probability density at V_0 = 0 (two-dimensional bulk thermophoresis). Dashed horizontal lines represent the steady-state maximal probability densities in the cold regions for (a) $V_0 = k_bT/0.15$ and (b) $V_0 = k_bT/0.4$.

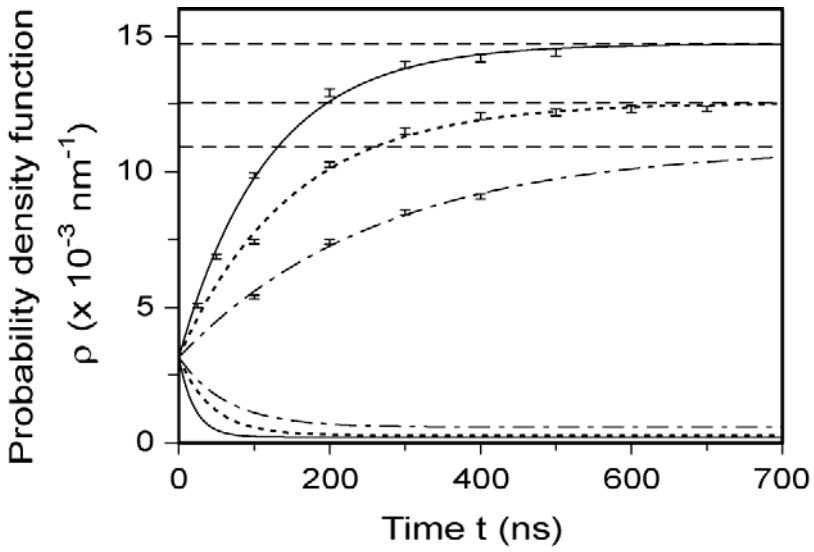

Figure. 3. The time evolution of the probability density in the cold (the upper curves) and hot (the lower curves) regions at different temperature modulations ΔT: 400 K (solid), 300 K (dotted), 200 K (dash-and-dotted); the other parameters are the same as for Fig. 2a. The error bars on the upper curves (concentration maximums) show the typical standard errors of the mean for the calculated points. Curve fitting was done assuming exponential dependencies.

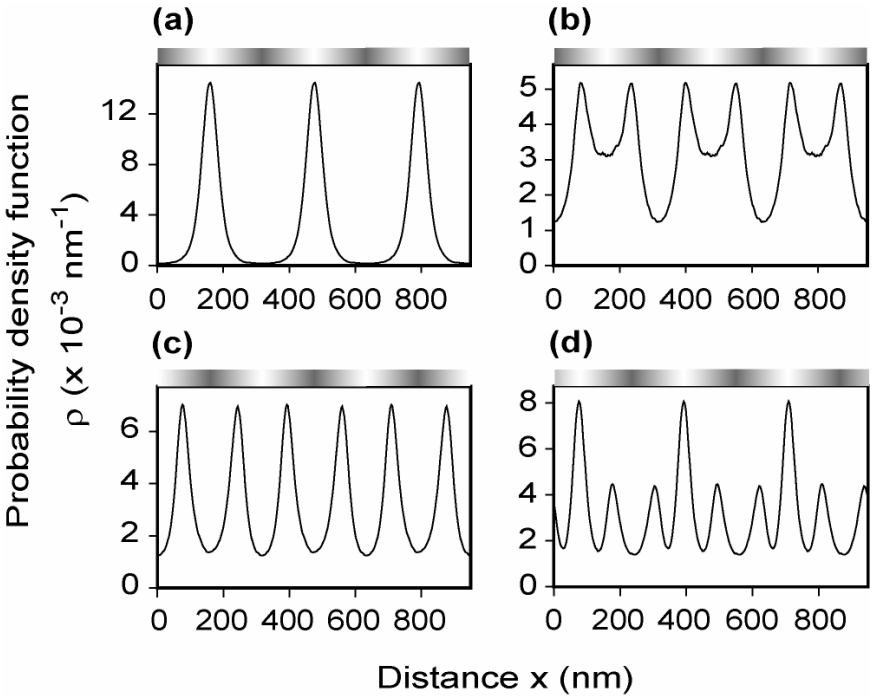

Figure 4. Superresolution technique in thermal tweezers. (a) The probability density function $\rho(x)$ identical to curve 1 in Fig. 2a (no superresolution). (b) $\rho(x)$ resulting from applying thermal tweezers to the uniform distribution of 50,000 non-interacting particles (in the $\lambda \times \lambda$ square with the periodic boundary conditions) at T_0 = 500 K, $V_0 = 500k_b/0.065$, ΔT = 800 K, λ = 316.4 nm, m = 100 a.u., a = 0.2 nm, $\gamma = 2.3\times10^{10}$ s^{-1} [15-18], and the evolution time t = 200 ns. (c) $\rho(x)$ obtained from the particle distribution in (b) by shifting the temperature modulation pattern by π and allowing the system to evolve for another 200 ns. (d) $\rho(x)$ obtained from the particle distribution in (c) by making T_0 = 300 K, further shifting the temperature modulation by $\approx \pi/2$ (so that the hot regions coincide with every second maximums in (c)), and allowing the system to evolve for 600 ns.